Jurnal Mandiri IT
Vol. 14 No. 2, October (2025), pp. 236-246

ISSN 2301-8984 (Print), 2809-1884 (Online)
Published by Institute of Computer Science

Analysis and design of an inset-feed microstrip antenna for a LEO satellite IoT ground station at 921 MHz

Rangga Taqwa[1], H.A. Danang Rimbawa[2], Apip Miptahudin[3], Bayu Nuar Khadapi Hasibuan[4], Aria Kusumah Sastradinata[5], Abbas Madani Bangun[6]
[1,2,3,4,5,6] Faculty of defense science and technology, Republic Indonesia Defence University, Bogor, Indonesia

ARTICLE INFO

Article history:

Received Sep 03, 2025
Revised Sep 20, 2025
Accepted Oct 22, 2025

Keywords:

Ansys HFSS;
Inset-Feed;
Link Budget;
LoRa;
Microstrip Antenna.

ABSTRACT

The evolution of the Internet of Things (IoT) demands global connectivity that terrestrial networks alone cannot provide1. Low Earth Orbit (LEO) satellites equipped with Long Range (LoRa) communication technology offer a promising solution to bridge this connectivity gap2. This paper presents a specific case study calculation for a LoRa-based IoT satellite mission, defining the system's operational constraints based on selected hardware3. This analysis is framed by the RFM95W LoRa transceiver for the ground station and the Satlab Polaris receiver for the satellite4. The datasheet specifications of these components establish the critical link parameters that dictate performance: a maximum Transmit Power (P_t)) of 20 dBm from the RFM95W 5and a Receiver Sensitivity threshold of -130 dBm for the Satlab Polaris6. The objectives are: (1) to conduct a comprehensive link budget analysis to validate the communication viability between a LEO satellite and a ground station 77, and (2) to design and predict the performance of an inset-feed microstrip antenna operating in the 920-925 MHz Indonesian LoRa frequency band using an FR-4 substrate. The detailed link budget analysis, performed for an uplink to a 500 km orbit 9, reveals that these specific parameters create a stringent performance requirement: while a reliable link margin of $+7.8 \text{ dB}$ is achieved at a 90° elevation (best case) 10101010, the system reaches its theoretical critical threshold (0.0 dB margin) at 19.1° and enters link failure with a -2.8 dB margin at the target 10° elevation. This failure is directly linked to the preliminary simulation of the initial antenna design, which shows a suboptimal return loss (S11) of -9.41 dB. This paper concludes that the system's target for low-elevation communication has not been met. The performance gap, defined by the hardware constraints, confirms that the initial antenna design is insufficient15. Therefore, systematic optimization of the antenna design is identified as the crucial next step to achieve a positive link margin at the 10° target elevation and ensure a robust communication link across all operational scenarios.

Corresponding Author:

Rangga Taqwa,
Faculty of Defense Engineering and Technology,
Republic Indonesia Defence University,
Kawasan IPSC., Bogor, 16810, Indonesia,
Email: ranngaalkhawarizmi@gmail.com.

1. INTRODUCTION

The global economy is experiencing a profound digital transformation, largely driven by the proliferation of the Internet of Things (IoT), which connects physical devices, vehicles, and appliances through sensors, software, and network connectivity, enabling autonomous data collection and exchange (Centenaro et al., 2021; Ogbodo et al., 2022). This paradigm shift is not just a technological upgrade but a fundamental enabler of new efficiencies, data-driven business models,

and improved decision-making across critical industries (Ram'irez-Arroyo et al., 2024). The value of IoT lies in its ability to provide real-time, granular data from previously unmonitored environments, unlocking unprecedented optimization and control (Lin et al., 2024).

Agriculture, Logistics, and Environmental MonitoringIn agriculture, IoT is revolutionizing "smart farming" or "precision agriculture" by deploying sensor networks, drones, and connected machinery to provide real-time insights into soil health, moisture, weather, and crop conditions (Mohamed et al., 2021; Yaacoub & Alouini, 2020). Automated irrigation systems, for example, can reduce water use by up to 50% (Centenaro et al., 2021)., while targeted fertilizer and pesticide applications minimize waste and environmental impact (McDonnell et al., 2024). IoT-based vehicle monitoring ensures optimal conditions for crops and livestock during transport and improves fuel efficiency (Ram'irez-Arroyo et al., 2024). The result is increased yields, optimized resource allocation, and more sustainable agricultural practices (Rolandi et al., 2021).

In logistics, IoT integration into vehicles, containers, and warehouses enables end-to-end, real-time supply chain visibility (Ding et al., 2020). GPS and location sensors allow dynamic route optimization, reducing delivery times, fuel consumption, and emissions (Zhang et al., 2021). Predictive maintenance, enabled by IoT sensors, prevents costly breakdowns and enhances fleet reliability (Ram'irez-Arroyo et al., 2024). RFID and barcode sensors automate inventory management, preventing overstocking or stockouts and transforming logistics into a proactive, data-driven discipline (Ding et al., 2020).

Environmental monitoring benefits from IoT through the deployment of low-power sensors across vast, remote areas, enabling continuous monitoring of air and water quality, detection of chemical spills, and flood risk management (Centenaro et al., 2021; Fraire et al., 2021). Automated alerts and emergency procedures can be triggered when thresholds are exceeded, preventing environmental disasters (Mohamed et al., 2021). The data collected supports regulatory compliance and sustainability initiatives (Gómez-Carmona et al., 2023).

The common thread in these applications is the foundational need for reliable, ubiquitous connectivity-without which the full potential of IoT cannot be realized (Centenaro et al., 2021; Ogbodo et al., 2022).

Despite the promise of a globally connected IoT ecosystem, a significant digital divide persists, with billions still offline, especially in rural and remote areas (Aruleba & Jere, 2022; Lin et al., 2024). Urban areas enjoy high connectivity, but less than half of rural populations have access, creating barriers to economic development and social inclusion (Morris et al., 2022; Tiwasing et al., 2022). The main obstacle is the high cost of extending terrestrial networks—fiber optics and cellular infrastructure—into sparsely populated, geographically challenging regions (Centenaro et al., 2021; Feurich et al., 2023). Low population density leads to low average revenue per user, making network expansion economically unviable (De Clercq et al., 2023). Additional challenges include unreliable power grids and limited road access, further complicating deployment and maintenance (Yaacoub & Alouini, 2020).

These techno-economic barriers create distinct connectivity voids in remote, rural, and maritime environments (Chaoub et al., 2020; Zhu & Jiang, 2022). In rural areas, lack of connectivity limits access to digital services like education, telemedicine, and commerce, perpetuating inequality (Esteban-Navarro et al., 2020; Philip & Williams, 2019). Even where cellular coverage exists, it is often unreliable and slow (Marshall, 2023). The maritime domain faces even greater challenges, as terrestrial networks do not extend far from the coast, leaving most of the world's oceans as connectivity deserts (Nomikos et al., 2022; Xia et al., 2020). Maritime operations, critical for global trade, rely on slow, expensive, and bandwidth-limited communication methods, further complicated by harsh weather (Fang et al., 2021; Saafi et al., 2022).

To bridge these gaps, integrated solutions combining terrestrial, satellite, and aerial networks are being developed (Centenaro et al., 2021; Ogbodo et al., 2022; Ram'irez-Arroyo et al., 2024). Multi-connectivity approaches, leveraging 5G, LPWAN, and low-earth-orbit satellites, are essential for providing reliable IoT connectivity in underserved regions (Callebaut et al., 2021; Fraire et al., 2021). Policy interventions, public-private partnerships, and innovative business models are also critical to ensure digital inclusion and sustainable development (Feurich et al., 2023; Gómez-Carmona et al., 2023).

While integrated LEO satellite and LoRa networks are recognized as a promising solution for these connectivity voids, a critical technical challenge remains in designing effective and low-cost ground station equipment. The viability of such a link, particularly to low-cost IoT devices, is heavily

dependent on the link budget. This budget is directly constrained by the performance of the ground station antenna, especially when tracking satellites at low elevation angles where path loss is greatest. Although many studies analyze LEO links , there is a specific research gap in designing and validating a low-cost microstrip antenna specifically for the Indonesian LoRa frequency (921 MHz) and quantitatively linking its preliminary performance back to the operational link margin of a realistic LEO-IoT system.

To address this gap, this paper presents a comprehensive design and analysis for a LEO-IoT ground station. The research has two specific objectives: (1) to conduct a detailed link budget analysis to define the minimum performance constraints for a viable communication link using specified hardware (RFM95W and Satlab Polaris) , and (2) to design and analyze the preliminary performance of a low-cost inset-feed microstrip antenna operating at 921 MHz on an FR-4 substrate.

The structure of this paper is as follows: Section 2 details the methodology, including the parameters and calculations for the link budget analysis and the initial design process for the microstrip antenna. Section 3 discusses the performance gap identified by the analysis and outlines the future work required for optimization. Finally, Section 4 provides the conclusion of this study.

2. METHODOLOGY

2.1 Link Budget Analysis: Detailed Calculation and Assumptions

Link budget analysis is a fundamental step to quantitatively validate communication links between ground stations and LEO satellites. The parameters considered include physical constants, hardware specifications, and engineering assumptions. The Earth's radius (6371 km) and LoRa frequency allocation (921 MHz) are fixed, while hardware parameters such as 20 dBm transmit power and −130 dBm receiver sensitivity are typically drawn from datasheets (Idmouida et al., 2022). Assumed parameters include a 500 km orbit altitude, which is typical for IoT and remote-sensing missions, feeder losses of 0.5 dB, and a transmit back-off of 0.5 dB to maintain linearity (Fang et al., 2021). The ground station antenna gain of 4 dBi and satellite antenna gain of 1 dBi represent typical values for patch and omnidirectional antennas (Fastenbauer et al., 2025). Atmospheric losses of 0.5 dB are included following ITU standards for sub-GHz frequencies (Giggenbach et al., 2023).

Calculations show that link margins transition from reliable (+7.8 dB) to critical (0 dB) and failure (−2.8 dB) as elevation decreases from 90° to 10°, which is consistent with previous studies demonstrating communication viability down to approximately 20° elevation (Aslnia et al., 2024; Fadilah et al., 2022; Gongora-Torres et al., 2022; Kim et al., 2023; Røste et al., 2023; Talgat et al., 2020).

Table 1. Parameters for Link Budget Calculation

Category	Parameter	Value	Source/Justification
CONSTANTS	Earth Radius (RE)	6371 km	A standard, fixed value for the mean radius of the Earth.
SPECIFICATIONS	Operating Frequency (f)	921 MHz	Regulatory allocation for LoRa in Indonesia.
	Transmit Power (Pt)	20 dBm	Specification: Maximum output power of the RFM95W LoRa module used in the ground station.
	Receiver Sensitivity	-130 dBm	Specification: Performance of the Satlab Polaris LoRa receiver on the satellite.
ASSUMPTIONS	Orbit Altitude (H)	500 km	Assumption: A typical LEO orbit altitude for IoT or observation missions .
	Feeder Losses (Lfeeder)	0.5 dB	Assumption: Estimated combined loss from cables and connectors at the ground station.
	Transmit Back-off (Lbackoff)	0.5 dB	Assumption: Power margin to ensure the transmitter operates in its linear region.
	Ground Station Antenna Gain (Gt)	4 dBi	Assumption: A typical theoretical gain for a single patch antenna on an FR-4 substrate before optimization.
	Satellite Antenna Gain (Gr)	1 dBi	Assumption: A typical gain for an omnidirectional antenna used on LEO satellites for wide coverage.
	Atmospheric Losses (Latmospheric)	0.5 dB	Assumption: A standard ITU recommendation for signal attenuation at sub-GHz frequencies .

This table provides a comprehensive list of all parameters used in the uplink link budget calculation, serving as the foundation for the analysis. It clearly distinguishes between fixed physical constants, parameters derived from the official specifications of the hardware (RFM95W and Satlab Polaris), and engineering assumptions made to model a realistic yet generalized LEO communication

scenario. This transparency is crucial for understanding the basis of the subsequent calculations and the resulting link margin.

Detailed Calculation Steps

The following steps detail the calculation of the *link budget* for different satellite elevation angles (ϵ).

1. Slant Range (d): This is the direct line-of-sight distance from the ground station to the satellite.
$$d = \sqrt{(R_E + H)^2 - (R_E \cos \vartheta)^2} - R_E \sin \theta \quad (1)$$

2. *Effective Isotropic Radiated Power (EIRP)*: This represents the total effective power transmitted from the ground station antenna.
$$\text{EIRP (dBm)} = P_t - L_{backoff} - L_{feeder} + G_t \quad (2)$$

3. *Free Space Path Loss (FSPL)*: This is the primary signal loss due to the spreading of the wave in free space.
$$Lfs(dB) = 20log10(dkm) + 20log10\,(fMHz) + 32.45 \quad (3)$$

4. Total Path Loss (Ltotal): This is the sum of *FSPL* and other atmospheric losses.
$$Ltotal = Lfs + Latmospheric \quad (4)$$

5. Received Power (Pr): This is the signal power arriving at the satellite's receiver antenna.
$$Pr(dBm) = EIRP - Ltotal + Gr \quad (5)$$

6. *Link Margin*: This is the crucial final value, representing the power surplus above the receiver's minimum sensitivity.
$$Link\ Margin\ (dB) = Pr - Receiver\ Sensitivity \quad (6)$$

2.2 Microstrip Antenna Design and Predictive Analysis

This section details the initial design process for the ground station antenna and analyzes its predicted performance before optimization.

Figure 1. Ansys Electronic Dekstop 2025 R1

Shows the layered construction typical of a microstrip antenna, which is fundamental to its operation and low-profile characteristics. The radiating element, or patch, is separated from the ground plane by the FR-4 dielectric substrate, which influences the antenna's resonant frequency and bandwidth. The inset-feed technique is highlighted, showing how the feedline is recessed into the patch to achieve the desired 50 Ω impedance match without external components.

The microstrip antenna design uses an inset-feed rectangular patch for the ground station. The FR-4 substrate (εr = 4.4, h = 1.6 mm) was chosen for cost-efficiency and mechanical robustness. Initial Dimension Calculation The antenna design began with analytical calculations to determine its initial physical dimensions. A notable discrepancy was observed: an online calculator design targeting 933 MHz was found to resonate at 921 MHz during preliminary HFSS simulation. This

highlights the difference between simplified analytical models and high-fidelity electromagnetic simulators, which more accurately account for effects like fringing fields.

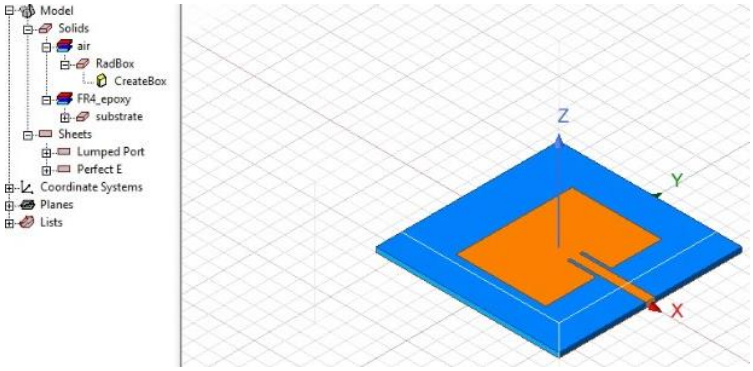

Figure 3. Structure of an Inset-Feed Microstrip Patch Antenna

Shows the layered construction typical of a microstrip antenna, which is fundamental to its operation and low-profile characteristics. The radiating element, or patch, is separated from the ground plane by the FR-4 dielectric substrate, which influences the antenna's resonant frequency and bandwidth. The inset-feed technique is highlighted, showing how the feedline is recessed into the patch to achieve the desired 50 Ω impedance match without external components.

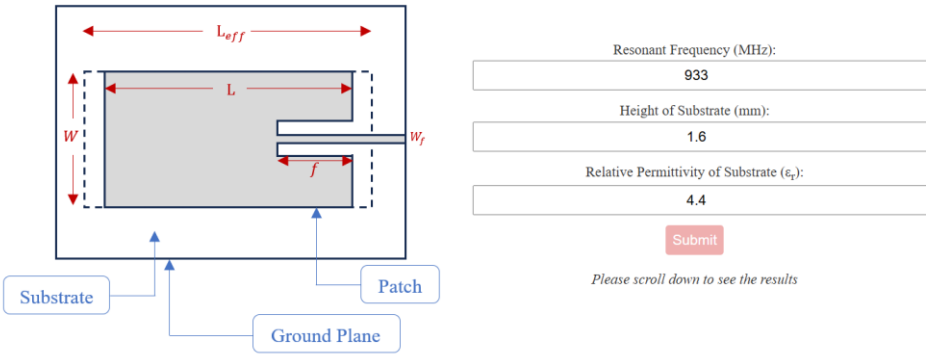

Calculated Values:

Parameter	Value
Width of Patch, W (mm)	97.843
Length of Patch, L (mm)	76.457
Approximate Feed Location from edge, f (mm)	24.896
Width of Feed Line, W_f (mm)	2.377
Effective Permittivity (ε_e)	4.254
Fringing Length, ΔL (mm)	0.745
Effective Length, L_{eff} (mm)	77.946
Edge Impedance (Ω)	312.927

Ref. for formulae: Constantine A. Balanis, *Antenna theory: Analysis and Design*, Third Edition, John Wiley & Sons, 2005

Figure 4. size calculation using the online inset-feed calculator

This figure displays the results of inset-feed antenna design calculator calculations which mark the beginning of the design process. The geometry, including the patch, substrate, and feed structure, is modeled precisely based on the initial theoretical calculations targeting a 933 MHz resonance. This model serves as the baseline for performance analysis, which revealed the actual resonance at 921 MHz and the need for subsequent optimization.

3. RESULT AND DISCUSSION

3.1 Link Budget Analysis Result

Applying the formulas from Section 2.1, the link budget was calculated for the best-case 90° and target worst-case $10° elevations.

- Slant Range (d):
  Calculation (90°):
  $d = 500$
  $d = 500\ km$
  Calculation (10°):
  $d \approx 1693.9$
  $d \approx 1693.9\ km$
- EIRP:
  Calculation: $EIRP = 20 - 0.5 - 0.5 + 4 = 23\ dBm$
- Free Space Path Loss (FSPL):
  Calculation (90°): $Lfs \approx 145.7\ Lfs \approx 145.7\ dB$
  Calculation (10°): $Lfs = 156.3\ Lfs = 156.3\ dB$
- Total Path Loss (LtotalLtotal):
  Calculation (90°): $Ltotal = 145.7 + 0.5 = 146.2\ dB$
  Calculation (10°): $Ltotal = 156.3 + 0.5 = 156.8\ dB$
- Received Power (Pr):
  Calculation (90°): $Pr = 23 - 146.2 + 1 = -122.2\ dBm$
  Calculation (10°): $Pr = 23 - 156.8 + 1 = -132.8\ dBm$
- Link Margin:
  Calculation (90°): $Link\ Margin = -122.2 - (-130) = +7.8\ dB$
  Calculation (10°): $Link\ Margin = -132.8 - (-130) = -2.8\ dB$

Analysis of Operational Range The point where communication is theoretically possible is when the Link Margin is 0 dB. By working backward from this condition, we can find the minimum operational elevation angle.

Analisis Operational Range :

Minimum Received Power (Pr,min*Pr,min*) : $-130\ dBm$
Maximum Total Loss (Ltotal,max*Ltotal*,*max*) : $23 - (-130) + 1 = 154\ dB$
Maximum FSPL (FSPLmax*FSPLmax*) : $154 - 0.5 = 153.5\ dB$
Maximum Slant Range (dmax*dmax*) :

$$From\ the\ FSPL\ formula,\ dmax \approx 1226.8\ dmax \approx 1226.8\ km$$

Minimum Elevation Angle (ϵmin*ϵmin*) :

$$From\ the\ slant\ range\ formula,\ \epsilon min \approx 19.1°\ \epsilon min \approx 19.1°$$

Table 2. Comparative Link Budget Analysis for Different Elevation Angles

Parameter	Elevation 90° (Best)	Elevation 19.1° (Minimal)	Elevation 10° (Failure)
Slant Range (d)	500 km	1226.8 km	1693.9 km
Total Loss (Ltotal)	146.2 dB	154.0 dB	156.8 dB
Received Power (Pr)	-122.2 dBm	-130.0 dBm	-132.8 dBm
Link Margin	+7.8 dB	0.0 dB	-2.8 dB
Communication Status	Reliable	Critical Threshold	Failure

This table summarizes the detailed link budget calculations for three critical elevation angles: 90° (best case), 19.1° (break-even point), and 10° (worst case). The results clearly demonstrate how the slant range dramatically increases as the elevation angle decreases, leading to a corresponding rise in path loss. The final link margin values explicitly show the transition from a reliable link, to a critical threshold, and finally to link failure, highlighting the system's operational limits.

3.2 Initial Antenna Simulation Results

A preliminary simulation of the initial design from Section 2.2 was conducted in Ansys HFSS. The test revealed a return loss (S11) of -9.41 dB at the resonant frequency of 921 MHz. This result indicates a poor impedance match, as a value greater than -10 dB is generally considered suboptimal. Based on this simulated S11 value, we can theoretically predict other performance metrics:

Simulation for the 2D and 3D radiation patterns has not yet been conducted. However, based on the fundamental theory of rectangular patch antennas, the radiation pattern is expected to be *broadside*, meaning the maximum radiation occurs perpendicular to the antenna's surface. The *gain* used in the *link budget* (4 dBi) remains a theoretical estimate that will be verified by comprehensive simulation in future work.

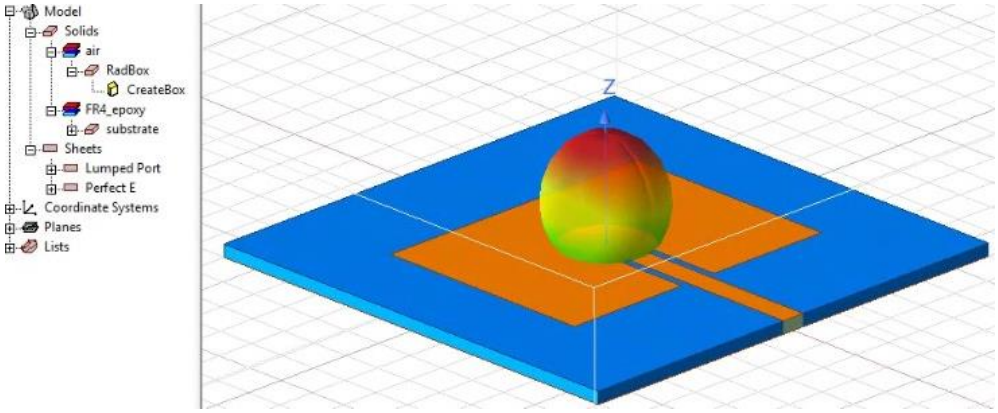

Figure 5. Theoretical 3D Radiation Pattern.

This image illustrates the expected shape of the antenna's radiation pattern, which is a critical performance characteristic for directional communication. As a typical rectangular patch antenna, it exhibits a broadside pattern, concentrating most of its radiated energy in a single lobe perpendicular to the patch surface. This directional characteristic is ideal for ground stations that point towards the sky, but the actual gain and beamwidth must be confirmed through future comprehensive simulations.

Discussion

Antenna design is a critical determinant of link reliability in LEO satellite-based IoT systems. Quantitative simulation results, particularly the interplay between S11 values, realized gain, and link margin, directly inform the system's ability to meet stringent link budget requirements for reliable communication.

Recent literature consistently highlights the importance of realistic modeling and hardware constraints in LEO satellite IoT links. Many studies employ stochastic geometry and analytical frameworks to estimate coverage probability, link availability, and the impact of system parameters such as antenna gain and path loss (Chan et al., 2020; Dong et al., 2025; Talgat et al., 2020; J. Zhou et al., 2024). However, these works often assume ideal or sufficiently high antenna gain, without explicitly addressing the practical limitations of low-cost, unoptimized antenna designs. For example, the critical elevation angle threshold for reliable LEO communication is frequently cited as ~20°, aligning with the calculated 19.1° threshold in the present analysis (Dwivedi et al., 2022; J. Zhou et al., 2024). This research advances the field by demonstrating, through direct simulation and link budget calculation, that a common FR-4 microstrip antenna with poor impedance matching (S11 = -9.41 dB) is the specific bottleneck causing link failure at low elevation angles, rather than the LoRa hardware or theoretical system limits.

The S11 parameter quantifies impedance matching; an S11 of -9.41 dB means 11.46% of transmitted power is reflected, not radiated (El-Din et al., 2022; Jia et al., 2022). This reflection loss directly reduces the realized antenna gain (Gt), which in turn lowers the link margin—each dB of gain lost translates to a dB reduction in link margin (Ghouse et al., 2024; X. Zhou et al., 2022). Simulation and measurement studies confirm that antennas with |S11| > 10 dB and high realized gain are essential for maintaining positive link margins, especially at low elevation angles where path loss is greatest (Ghouse et al., 2024; Wu et al., 2015). For instance, a -2.8 dB link margin at 10° elevation is not a theoretical limit but a direct result of the suboptimal S11 and associated gain loss.

Parameter	Impact on Link Margin	Practical Implication	Citations
S11 (Impedance)	Poor S11 increases power reflection	Reduces realized gain, link margin	671318
Realized Gain	Directly adds to link budget	Essential for overcoming path loss	111318
Link Margin	Must be >0 dB for reliable comms	Negative margin = link failure	

The findings underscore that using standard analytical formulas without optimizing antenna design can result in system failure at low elevation angles, even if all other hardware meets specifications (Ghouse et al., 2024; Wu et al., 2015). This highlights the necessity for systematic antenna optimization—improving S11 and realized gain is not just beneficial but essential for reliable LEO IoT communication, especially in cost-sensitive or mass-deployed ground stations.

This establishes a clear and critical path for future work. The current design is a validated starting point, but it is not a final solution. The next phase of this research must focus on systematic optimization.

Optimization and Validation Plan

The following steps are planned to develop a viable antenna design:

1. Systematic Optimization: A *parametric sweep* will be performed in *Ansys HFSS*. Key geometric variables, primarily the patch length (to fine-tune the resonant frequency) and the inset depth and gap (to achieve an optimal 50 Ω impedance match), will be varied. The optimization goal will be to minimize the *S11* parameter to a target of less than -15 dB, which corresponds to a *VSWR* below 1.5:1.
2. Comprehensive Simulation: Once an optimized geometry is found, a full simulation will be executed. This will provide accurate, simulated data for all key performance indicators, including the final S11, VSWR, 2D and 3D radiation patterns, peak realized gain, and input impedance.
3. Link Budget Re-evaluation: The new, accurate gain value obtained from the optimized simulation will be substituted back into the link budget calculation. The analysis will be repeated to verify if the optimized antenna can produce a positive and healthy link margin (target > 3 dB) across the entire operational range, especially at the critical low elevation angles.

4. CONCLUSION

This research has successfully conducted a foundational analysis for a LoRa-based IoT communication system intended for a LEO satellite mission. The detailed link budget analysis for the uplink from a ground station to a satellite at a 500 km altitude reveals that the system is highly sensitive to antenna performance . Using a standard patch antenna with an assumed theoretical gain of 4 dBi, the communication link fails at low elevation angles (below 19.1°), resulting in a negative link margin of -2.8 dB at 10°. The initial design of an inset-feed microstrip patch antenna successfully resonates at the target frequency of 921 MHz, but preliminary simulations show a suboptimal impedance match (S11 = -9.41 dB). This confirms that while the design approach is valid, the initial performance is insufficient for a robust communication system.The scientific contribution of this paper is the quantitative identification of the unoptimized, low-cost FR-4 antenna—rather than the LoRa hardware—as the specific bottleneck causing link failure at the critical elevation threshold. The practical implication for strengthening connectivity in remote areas is direct: it confirms that affordable LEO-IoT ground stations are a viable path, but only if systematic antenna optimization is prioritized to close this identified performance gap. Therefore, the clear conclusion is that this performance gap must be closed. Future work will proceed beyond preliminary analysis. The immediate next step is using Ansys HFSS to optimize the antenna's geometry to improve its impedance match (target S11 < -15 dB) and maximize its realized gain7. Following this, more specific research will involve experimental validation: (1) fabricating the optimized antenna prototype, (2) measuring its performance (S11 and radiation pattern) using a VNA and anechoic chamber, and (3) conducting field testing to confirm a robust, positive link margin across all operational scenarios in an end-to-end test with a LEO satellite.

ACKNOWLEDGEMENTS

All praises be to God Almighty for His grace and blessings, which made the completion of this research possible. The author extends sincere gratitude to the Satellite Technology Research Center

(PRTS) BRIN and the Republic of Indonesia Defense University (UNHAN) for facilitating this practical work.
Special appreciation is to Kolonel Laut (E) Dr. H.A. Danang Rimbawa, S.Si., M.T., M.Tr.Opsla., for his constructive feedback and motivation.

REFERENCES

Aruleba, K., & Jere, N. (2022). Exploring Digital Transforming Challenges in Rural Areas of South Africa through a Systematic Review of Empirical Studies. *Scientific African*. https://doi.org/10.1016/j.sciaf.2022.e01190

Aslnia, M., Soleimani, M., Sedighy, S. H., & Ebrahimi, A. (2024). Statistical channel modeling for low-elevation in LEO satellite communication. *Results in Engineering*, *23*, 102494.

Callebaut, G., Leenders, G., Van Mulders, J., Ottoy, G., Strycker, L., & Perre, L. (2021). The Art of Designing Remote IoT Devices—Technologies and Strategies for a Long Battery Life. *Sensors (Basel, Switzerland)*, *21*. https://doi.org/10.3390/s21030913

Centenaro, M., Costa, C. E., Granelli, F., Sacchi, C., & Vangelista, L. (2021). A survey on technologies, standards and open challenges in satellite IoT. *IEEE Communications Surveys & Tutorials*, *23*(3), 1693–1720.

Chan, C., Al-Hourani, A., Choi, J., Gomez, K., & Kandeepan, S. (2020). Performance Modeling Framework for IoT-over-Satellite Using Shared Radio Spectrum. *Remote. Sens.*, *12*, 1666. https://doi.org/10.3390/rs12101666

Chaoub, A., Giordani, M., Lall, B., Bhatia, V., Kliks, A., Mendes, L., Rabie, K. M., Saarnisaari, H., Singhal, A., Zhang, N., & Dixit, S. (2020). 6G for Bridging the Digital Divide: Wireless Connectivity to Remote Areas. *IEEE Wireless Communications*, *29*, 160–168. https://doi.org/10.1109/mwc.001.2100137

De Clercq, M., D'haese, M., & Buysse, J. (2023). Economic growth and broadband access: The European urban-rural digital divide. *Telecommunications Policy*. https://doi.org/10.1016/j.telpol.2023.102579

Ding, Y., Jin, M., Li, S., & Feng, D. (2020). Smart logistics based on the internet of things technology: an overview. *International Journal of Logistics Research and Applications*, *24*, 323–345. https://doi.org/10.1080/13675567.2020.1757053

Dong, W.-Y., Yang, S., Zhang, P., & Chen, S. (2025). Modeling and Performance Analysis of IoT-Over-LEO Satellite Systems Under Realistic Operational Constraints: A Stochastic Geometry Approach. *IEEE Internet of Things Journal*, *12*, 30576–30593. https://doi.org/10.1109/jiot.2025.3570843

Dwivedi, A., Chaudhari, S., Varshney, N., & Varshney, P. (2022). Performance Analysis of LEO Satellite-Based IoT Networks in the Presence of Interference. *IEEE Internet of Things Journal*, *11*, 8783–8799. https://doi.org/10.1109/jiot.2023.3321574

El-Din, M., Shams, S., Allam, A., Gaafar, A., Elhennawy, H., & Sree, M. F. A. (2022). SIGW Based MIMO Antenna for Satellite Down-Link Applications. *IEEE Access*, *10*, 35965–35976. https://doi.org/10.1109/access.2022.3160473

Esteban-Navarro, M.-Á., García-Madurga, M.-Á., Morte-Nadal, T., & Nogales-Bocio, A.-I. (2020). The rural digital divide in the face of the COVID-19 pandemic in Europe—recommendations from a scoping review. *Informatics*, *7*(4), 54.

Fadilah, N., Arifin, M. A., Qonita, A. H., Najati, N., Pratomo, B., & Nasser, E. N. (2022). Link and Doppler analysis for LEO constellation space-based IoT. *2022 IEEE International Conference on Aerospace Electronics and Remote Sensing Technology (ICARES)*, 1–6.

Fang, X., Feng, W., Wang, Y., Chen, Y., Ge, N., Ding, Z., & Zhu, H. (2021). NOMA-Based Hybrid Satellite-UAV-Terrestrial Networks for 6G Maritime Coverage. *IEEE Transactions on Wireless Communications*, *22*, 138–152. https://doi.org/10.1109/twc.2022.3191719

Fastenbauer, A., Kaneko, M., Svoboda, P., & Rupp, M. (2025). Impact of Elevation Angle on Multi-Beam LEO Satellite Communication Systems. *IEEE Access*.

Feurich, M., Kouřilová, J., Pělucha, M., & Kasabov, E. (2023). Bridging the urban-rural digital divide: taxonomy of the best practice and critical reflection of the EU countries' approach. *European Planning Studies*, *32*, 483–505. https://doi.org/10.1080/09654313.2023.2186167

Fraire, J., Iova, O.-T., & Valois, F. (2021). Space-Terrestrial Integrated Internet of Things: Challenges and Opportunities. *IEEE Communications Magazine*, *60*, 64–70. https://doi.org/10.1109/mcom.008.2200215

Ghouse, P. S. B., Mane, P., Ali, T., Dattathreya, G. S. G., Gopi, S. P., Pathan, S., & Anguera, J. (2024). A Low-Profile Circularly Polarized Millimeter-Wave Broadband Antenna Analyzed with a Link Budget for IoT Applications in an Indoor Scenario. *Sensors (Basel, Switzerland)*, *24*. https://doi.org/10.3390/s24051569

Giggenbach, D., Knopp, M. T., & Fuchs, C. (2023). Link budget calculation in optical LEO satellite downlinks with on/off-keying and large signal divergence: A simplified methodology. *International Journal of Satellite Communications and Networking*, *41*(5), 460–476.

Gómez-Carmona, O., Buján-Carballal, D., Casado-Mansilla, D., López-de-Ipiña, D., Cano-Benito, J., Cimmino, A., Poveda-Villalón, M., García-Castro, R., Almela-Miralles, J., & Apostolidis, D. (2023). Mind the gap: The AURORAL ecosystem for the digital transformation of smart communities and rural areas. *Technology in Society*, *74*, 102304.

Gongora-Torres, J. M., Vargas-Rosales, C., Aragón-Zavala, A., & Villalpando-Hernandez, R. (2022). Link budget analysis for LEO satellites based on the statistics of the elevation angle. *Ieee Access*, *10*, 14518–14528.

Idmouida, H., Minaoui, K., & Guennoun, Z. (2022). Link Budget Analysis for a 3U Nanosatellite Operating At S-band. *2022 IEEE International Conference on Communication, Networks and Satellite (COMNETSAT)*, 27–32.

Jia, H., Ni, Z., Jiang, C., Kuang, L., & Lu, J. (2022). Uplink Interference and Performance Analysis for Megasatellite Constellation. *IEEE Internet of Things Journal*, *9*, 4318–4329. https://doi.org/10.1109/jiot.2021.3104095

Kim, E., Roberts, I. P., & Andrews, J. G. (2023). Downlink analysis and evaluation of multi-beam LEO satellite communication in shadowed Rician channels. *IEEE Transactions on Vehicular Technology*, *73*(2), 2061–2075.

Lin, H., Kishk, M. A., & Alouini, M.-S. (2024). Performance evaluation of rf-powered iot in rural areas: The wireless power digital divide. *IEEE Transactions on Green Communications and Networking*, *8*(2), 716–729.

Marshall, A. (2023). A new rural digital divide? Taking stock of geographical digital inclusion in Australia. *Media International Australia*, *190*, 68–84. https://doi.org/10.1177/1329878x231202274

McDonnell, K., Palattella, M. R., Awan, M. F., Pradas, D., Camacho, F., Nørremark, M., & Krčo, S. (2024). Integrated Networks and Services for Sustainable Rural Digitalization. *2024 IEEE International Humanitarian Technologies Conference (IHTC)*, 1–7.

Mohamed, E. S., Belal, A., Abd-Elmabod, S. K., El-Shirbeny, M., Gad, A., & Zahran, M. (2021). Smart farming for improving agricultural management. *The Egyptian Journal of Remote Sensing and Space Science*. https://doi.org/10.1016/j.ejrs.2021.08.007

Morris, J., Morris, W., & Bowen, R. (2022). Implications of the digital divide on rural SME resilience. *Journal of Rural Studies*, *89*, 369–377.

Nomikos, N., Gkonis, P. K., Bithas, P. S., & Trakadas, P. (2022). A survey on UAV-aided maritime communications: Deployment considerations, applications, and future challenges. *IEEE Open Journal of the Communications Society*, *4*, 56–78.

Ogbodo, E., Abu-Mahfouz, A., & Kurien, A. (2022). A Survey on 5G and LPWAN-IoT for Improved Smart Cities and Remote Area Applications: From the Aspect of Architecture and Security. *Sensors (Basel, Switzerland)*, *22*. https://doi.org/10.3390/s22166313

Philip, L., & Williams, F. (2019). Remote rural home based businesses and digital inequalities: Understanding needs and expectations in a digitally underserved community. *Journal of Rural Studies*. https://doi.org/10.1016/j.jrurstud.2018.09.011

Ram'irez-Arroyo, A., L'opez, M., Rodr'iguez, I., Damsgaard, S., & Mogensen, P. (2024). Multi-connectivity solutions for rural areas: Integrating terrestrial 5G and satellite networks to support innovative IoT use cases. *Smart Agricultural Technology*. https://doi.org/10.1016/j.atech.2025.101260

Rolandi, S., Brunori, G., Bacco, M., & Scotti, I. (2021). The Digitalization of Agriculture and Rural Areas: Towards a Taxonomy of the Impacts. *Sustainability*, *13*, 5172. https://doi.org/10.3390/su13095172

Røste, T., Yang, K., & Wen, C. (2023). Satellite to buoy IoT communications in the Arctic Ocean. *Frontiers in Marine Science*, *10*, 1153798.

Saafi, S., Vikhrova, O., Fodor, G., Hosek, J., & Andreev, S. (2022). AI-Aided Integrated Terrestrial and Non-Terrestrial 6G Solutions for Sustainable Maritime Networking. *IEEE Network*, *36*,

183–190. https://doi.org/10.1109/mnet.104.2100351
Talgat, A., Kishk, M. A., & Alouini, M.-S. (2020). Stochastic geometry-based analysis of LEO satellite communication systems. *IEEE Communications Letters*, *25*(8), 2458–2462.
Tiwasing, P., Clark, B., & Gkartzios, M. (2022). How can rural businesses thrive in the digital economy? A UK perspective. *Heliyon*, *8*. https://doi.org/10.1016/j.heliyon.2022.e10745
Wu, J., Cheng, Y., & Fan, Y. (2015). A Wideband High-Gain High-Efficiency Hybrid Integrated Plate Array Antenna for V-Band Inter-Satellite Links. *IEEE Transactions on Antennas and Propagation*, *63*, 1225–1233. https://doi.org/10.1109/tap.2014.2382664
Xia, T., Wang, M., Zhang, J., & Wang, L. (2020). Maritime Internet of Things: Challenges and Solutions. *IEEE Wireless Communications*, *27*, 188–196. https://doi.org/10.1109/mwc.001.1900322
Yaacoub, E., & Alouini, M.-S. (2020). A key 6G challenge and opportunity—Connecting the base of the pyramid: A survey on rural connectivity. *Proceedings of the IEEE*, *108*(4), 533–582.
Zhang, Y., Love, D., Krogmeier, J., Anderson, C., Heath, R., & Buckmaster, D. (2021). Challenges and Opportunities of Future Rural Wireless Communications. *IEEE Communications Magazine*, *59*, 16–22. https://doi.org/10.1109/mcom.001.2100280
Zhou, J., Wang, R., Shihada, B., & Alouini, M. (2024). End-to-End Uplink Performance Analysis of Satellite-Based IoT Networks: A Stochastic Geometry Approach. *IEEE Open Journal of the Communications Society*, *5*, 4036–4045. https://doi.org/10.1109/ojcoms.2024.3422110
Zhou, X., Ying, K., Gao, Z., Wu, Y., Xiao, Z., Chatzinotas, S., Yuan, J., & Ottersten, B. (2022). Active Terminal Identification, Channel Estimation, and Signal Detection for Grant-Free NOMA-OTFS in LEO Satellite Internet-of-Things. *IEEE Transactions on Wireless Communications*, *22*, 2847–2866. https://doi.org/10.1109/twc.2022.3214862
Zhu, X., & Jiang, C. (2022). Integrated Satellite-Terrestrial Networks Toward 6G: Architectures, Applications, and Challenges. *IEEE Internet of Things Journal*, *9*, 437–461. https://doi.org/10.1109/jiot.2021.3126825